

# *A self-assembling fluorescent dipeptide conjugate for cell labelling*

Article

Published Version

Creative Commons: Attribution 4.0 (CC-BY)

Kirkham, S., Hamley, I. W. ORCID: <https://orcid.org/0000-0002-4549-0926>, Smith, A. M., Gouveia, R. M., Connon, C. J., Reza, M. and Ruokolainen, J. (2016) A self-assembling fluorescent dipeptide conjugate for cell labelling. *Colloids and Surfaces B: Biointerfaces*, 137. pp. 104-108. ISSN 0927-7765 doi: <https://doi.org/10.1016/j.colsurfb.2015.04.062> Available at <https://centaur.reading.ac.uk/41591/>

It is advisable to refer to the publisher's version if you intend to cite from the work. See [Guidance on citing](#).

Published version at: <http://dx.doi.org/10.1016/j.colsurfb.2015.04.062>

To link to this article DOI: <http://dx.doi.org/10.1016/j.colsurfb.2015.04.062>

Publisher: Elsevier

All outputs in CentAUR are protected by Intellectual Property Rights law, including copyright law. Copyright and IPR is retained by the creators or other copyright holders. Terms and conditions for use of this material are defined in the [End User Agreement](#).

[www.reading.ac.uk/centaur](http://www.reading.ac.uk/centaur)

**CentAUR**

Central Archive at the University of Reading

Reading's research outputs online



Contents lists available at ScienceDirect

## Colloids and Surfaces B: Biointerfaces

journal homepage: [www.elsevier.com/locate/colsurfb](http://www.elsevier.com/locate/colsurfb)



### A self-assembling fluorescent dipeptide conjugate for cell labelling

Steven Kirkham<sup>a</sup>, Ian W. Hamley<sup>a,\*</sup>, Andrew M. Smith<sup>a,1</sup>, Ricardo M. Gouveia<sup>b</sup>,  
Che J. Connon<sup>b</sup>, Mehedi Reza<sup>c</sup>, Janne Ruokolainen<sup>c</sup>

<sup>a</sup> School of Chemistry, Pharmacy and Food Biosciences, University of Reading, Whiteknights, Reading RG6 6AD, UK

<sup>b</sup> Institute of Genetic Medicine, Newcastle University, International Centre for Life, Central Parkway, Newcastle upon Tyne NE1 3BZ, UK

<sup>c</sup> Department of Applied Physics, Aalto University School of Science, P.O. Box 15100, FI-00076 Aalto, Finland

#### ARTICLE INFO

##### Article history:

Received 28 February 2015  
Received in revised form 27 April 2015  
Accepted 28 April 2015  
Available online xxx

##### Keywords:

Peptides  
Peptide conjugates  
Self-assembly  
Fluorescence

#### ABSTRACT

Derivatives of fluorophore FITC (fluorescein isothiocyanate) are widely used in bioassays to label proteins and cells. An N-terminal leucine dipeptide is attached to FITC, and we show that this simple conjugate molecule is cytocompatible and is uptaken by cells (human dermal and corneal fibroblasts) in contrast to FITC itself. Co-localisation shows that FITC-LL segregates in peri-nuclear and intracellular vesicle regions. Above a critical aggregation concentration, the conjugate is shown to self-assemble into beta-sheet nanostructures comprising molecular bilayers.

© 2015 The Authors. Published by Elsevier B.V. This is an open access article under the CC BY license (<http://creativecommons.org/licenses/by/4.0/>).

N-terminally attached aromatic substituents can be employed to drive the self-assembly of peptides via aromatic stacking interactions and/or hydrophobic effects. Commonly used moieties include Fmoc [9-fluorenylmethoxycarbonyl chloride] [1–9], Boc [*tert*-butyloxycarbonyl] [2,10,11], naphthalene [12–14], pyrene [15–17] or naproxen [18].

These conjugates have potential in biomedical applications, either directly due to the incorporation of responsive amino acids [19] or via the attachment of functional units such as NSAIDs (nonsteroidal anti-inflammatory drugs) for example naproxen as N-terminal aromatic units [20,21] or laterally, e.g. side-chain attached taxol [22] among other therapeutic agents [23]. Enzymatic hydrogelation also has potential in the development of biomaterials such as cell culture matrices or supports [8,24–27]. In one example of the former category, it has been shown that the naphthyl-tetrapeptide Nap-FFK(fluoro)Y(Phos) [K(fluoro) denotes lysine labelled with a fluorophore and Y(Phos) indicates phosphorylated tyrosine] can self-assemble intracellularly due to enzymatic dephosphorylation of the tyrosine [19]. The fluorophore enables the imaging of the peptide aggregates uptaken by cells [19].

A FITC-labelled cell-penetrating peptide has been developed based on a sequence from the N-terminal region of the X-protein of the hepatitis B virus [28]. The peptide, called Xentry, was able to kill melanoma cells and has potential in other drug delivery applications. As well as a fluorescence tag for many proteins and peptides [29–32], FITC has also been used to label inorganic [33,34] or polymer nanoparticles [35,36] or synthetic polymers [37,38] for cell uptake and labelling studies. FITC-labelled casein is widely used in assays for proteolytic enzymes [39].

In the present paper we investigate the cell labelling abilities of a peptide amphiphile containing the bulky hydrophobic fluorophore, FITC at the N-terminus. The FITC moiety is attached to a di-leucine model peptide. This PA was designed as a potential biocompatible fluorescent label. As such, FITC-LL was examined by fluorescence microscopy for its ability to be uptaken by human fibroblasts in vitro while preserving high cell viability. Interestingly, the dipeptide modification of FITC-LL was shown to be necessary and sufficient for improved cell internalisation compared with the non-conjugated FITC molecule. In this perspective, the FITC-LL conjugate proves a simple peptide-based fluorescent label with the potential for further peptide functionalisation for applications in delivery or diagnostics. Although FITC derivatives have been prepared as sensitive fluorescent probes in living cells [40], to the best of our knowledge, the observation of cell uptake by a FITC-peptide conjugate with such a short peptide attached, is unprecedented. We also show that at higher concentration, above a critical aggregation concentration, FITC-LL undergoes self-assembly into nanotape structures.

\* Corresponding author. Tel.: +44 118 378 6341; fax: +44 118 378 8454.

E-mail address: [I.W.Hamley@reading.ac.uk](mailto:I.W.Hamley@reading.ac.uk) (I.W. Hamley).

<sup>1</sup> Current address: School of Materials, The University of Manchester, Manchester M13 9PL, UK.

<http://dx.doi.org/10.1016/j.colsurfb.2015.04.062>

0927-7765/© 2015 The Authors. Published by Elsevier B.V. This is an open access article under the CC BY license (<http://creativecommons.org/licenses/by/4.0/>).

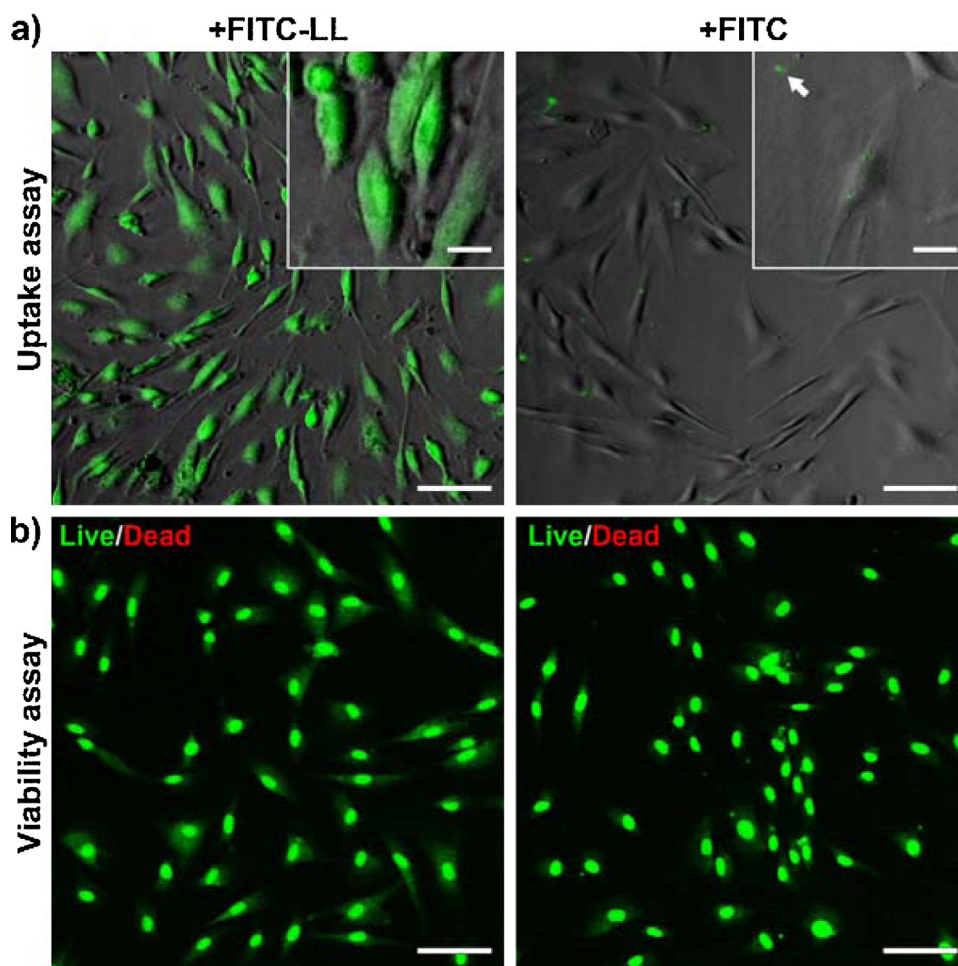


**Fig. 1.** Internalisation and cytocompatibility of FITC-LL in cultures of human fibroblasts. Cells incubated for 24 h with  $7.5 \times 10^{-3}$  wt% of FITC-LL (left) or FITC (right panels) were imaged by (a) bright-field and fluorescence microscopy to determine the extent of fluorophore internalisation (green), or (b) subjected to a Live/Dead cell double staining assay to determine the impact of fluorophore intake on cell viability. Scale bars = 100  $\mu\text{m}$  (panels) or 20  $\mu\text{m}$  (insets). (For interpretation of the references to color in this figure legend, the reader is referred to the web version of this article.)

To evaluate the ability of FITC-LL to be internalised, the conjugate was incubated at  $7.5 \times 10^{-3}$  wt% with human fibroblast cultures *in vitro*. In these experiments, the cellular uptake of FITC-LL was directly observed by microscopy through the intrinsic green fluorescence of the conjugate (Fig. 1). After a 24-h incubation period, FITC-LL was shown to mark the majority of cells, indicating high cellular uptake (Fig. 1a, left panel), despite being at a lower molar concentration.

FITC-LL was predominantly found intracellularly, with almost no green fluorescence detected outside the cells (Fig. 1a, inset). In contrast, cultures incubated with  $7.5 \times 10^{-3}$  wt% of the non-conjugated, highly-fluorescent FITC presented almost no green-positive cells (Fig. 1a, right panel). Moreover, signals corresponding to FITC were mostly found outside cells, appearing as precipitated aggregates on the surface of the tissue culture flask (Fig. 1a, right inset, arrow).

Furthermore, FITC-LL was shown to be highly cytocompatible. Cultures incubated with FITC-LL or FITC were analysed by fluorescence microscopy using a Live/Dead cell Double Staining kit to assess the number of live (green, Cyto-Dye-positive) and dead (red, propidium iodide-positive) cells (Fig. 1b). The results showed that, despite being profusely internalised, FITC-LL maintained very high cell viability (Fig. 1b, left panel). Moreover, this level of cytocompatibility was comparable to that of the non-internalised FITC (Fig. 1b, right panel). Although FITC and FITC-LL exhibit green fluorescence (similar to that of the Cyto dye in the assay), had significant cell

death been observed then a mixture of red and green fluorescence would have been observed. Taken together, these results demonstrate that the modification of FITC to include two leucine residues greatly improves its capacity to be taken up by cells without compromising cell viability. As such, FITC-LL represents a facile new system for fluorescence labelling of cells.

To further characterise the internalisation of FITC-LL, cells incubated for 24 h with the green-fluorescent conjugate were also stained at the nucleus using the fluorescent DNA stain DAPI (4',6-diamidino-2-phenylindole) (Fig. 2, blue). The results showed that FITC-LL was particularly concentrated in the peri-nuclear region of cells (Fig. 2a, light blue staining) and inside vesicle-shaped intracellular compartments (Fig. 2b, arrows) (see SI Fig. 2 for the separate fluorescence colour channel images). Cells showing more pronounced peri-nuclear accumulation of FITC-LL showed fewer green-positive vesicle compartments (Fig. 2 and SI Fig. 3). Assuming that cultures were constituted by a homogeneous population of cells, the different FITC-LL intracellular localisation might be due to differences in (1) the rate of intake and clearance of the conjugate, (2) the physiological state of the cell, and/or (3) nuclear membrane permeability.

In addition to its bioactivity at low concentration, we found via a fluorescence assay that FITC-LL exhibits a critical aggregation concentration, *cac* (Fig. 3), at a concentration of  $(0.23 \pm 0.02)$  wt%, i.e. significantly above the concentration at which the cell fluorescence studies were performed. The corresponding fluorescence emission

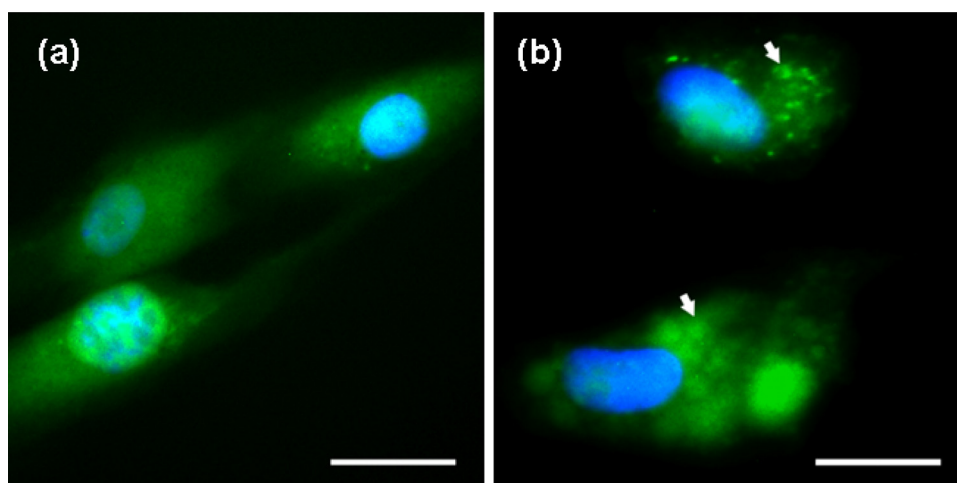


**Fig. 2.** Fluorescence microscope images of human corneal fibroblasts from intracellular localisation experiments using DAPI (blue) as a nuclear stain. The FITC-LL (green fluorescence) is localised in the peri-nuclear region (a) or in intra-cellular vesicles (arrows in part b). The scale bars correspond to 20  $\mu\text{m}$ . (For interpretation of the references to color in this figure legend, the reader is referred to the web version of this article.)

spectra are shown in SI Fig. 4. Self-quenching is believed to reduce the fluorescence at high concentration, in the self-assembled state.

We therefore examined the nature of the self-assembled nanostructure above the *cac*, including examination of any secondary structure via spectroscopic methods, as well as the morphology via electron microscopy and X-ray scattering techniques.

The secondary structure of FITC-LL was probed using Fourier Transform Infra-Red (FTIR) spectroscopy. Fig. 4a shows spectra in the amide I region. A peak at  $1633\text{ cm}^{-1}$  indicates that FITC-LL adopts a  $\beta$ -sheet structure [41,42]. There is also a strong peak in the amide II region at  $1578\text{ cm}^{-1}$ , which is due to N–H bend/C–N stretch deformations [41]. The circular dichroism (CD) spectrum in Fig. 4b does not resemble that typically associated with a  $\beta$ -sheet structure, usually expected to present a positive maximum near 200 nm and a negative minimum near 216 nm [43]. However, the spectrum may be influenced by the UV absorbance of the FITC moiety [44,45] and/or significant light scattering due to the formation of extended nanostructures. To examine any chiral ordering of the FITC moiety, the spectrum was measured up to 550 nm and indeed a broad peak is observed around the expected maximum near 520 nm [44,45].

The self-assembly of FITC-LL into sheet-like structures was revealed by cryogenic transmission electron microscopy (cryo-TEM). Representative images are shown in Fig. 5 and SI Fig. 5. These

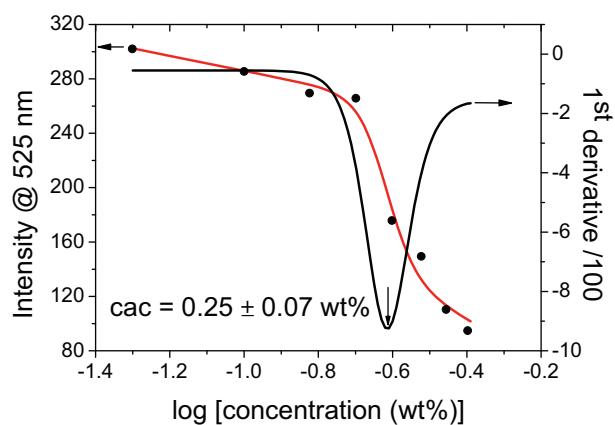


**Fig. 3.** Concentration dependence of fluorescence emission intensity for FITC shows a break point at 0.25 wt%, which corresponds to a critical aggregation concentration. Details of the sigmoidal fitting function are provided in the SI.

reveal the presence of thin sheets (the edges of some curled-up sheets can be seen, indicating the small thickness) with a dispersity in width. To the best of our knowledge, sheet-like structures have not previously been reported for dipeptide conjugates with bulky aromatic substituents.

To complement cryo-TEM, and to provide detailed in situ structural information, self-assembled FITC-LL nanostructures were analysed by small-angle X-ray scattering (SAXS). The SAXS intensity profile measured from a 0.5 wt% solution is shown in Fig. 6, along with a fit to a model form factor profile. The form factor was that for a Gaussian bilayer, which is consistent with the sheet structures observed by cryo-TEM (Fig. 5), and which clearly fits the data very well. We have used this form factor previously to fit SAXS data from layered peptide assemblies [46–48]. It consists of a sum of three Gaussian functions which parameterize the electron density profile across a lipid (or lipopeptide) bilayer – with two Gaussian functions representing the positive electron density regions associated with the headgroups and one representing the negative relative electron density region of the lipid chains. In the case of FITC-LL, although a “bilayer” is not expected, we can use the same electron density profile for the expected monolayer since the inner leaflet is expected to be the FITC-LL moieties, with the LL residues comprising the exterior leaflets, on each side of the interior dense FITC region. The fitting of the data in Fig. 6 was performed using SASfit [49], and indicated a layer thickness  $t = 8.9\text{ \AA}$  (with 11% polydispersity, defined as the Gaussian half-width at half-maximum). The other fit parameters were the relative electron densities, i.e. the heights of the Gaussian functions representing the lipid core  $\rho_c = -2.36 \times 10^{-5}$  and headgroup regions  $\rho_h = 6.4 \times 10^{-6}$  as well as a flat background  $B = 0.0004$ . The widths of the Gaussian functions were fixed at  $5\text{ \AA}$ , the bilayer radius was fixed at  $500\text{ \AA}$  (since  $D \gg t$ , this only provides a scaling factor) and the overall scaling factor was  $F = 0.001$ . The determined layer thickness  $t = 8.9\text{ \AA}$  indicates interdigitation of molecules within the layer, since the estimated molecular length is around this value.

In summary, the conjugate FITC-LL was synthesized, incorporating the fluorophore fluorescein isothiocyanate attached N-terminally to dileucine. A fluorescence assay reveals a critical aggregation concentration, above which the fluorescence emission intensity is reduced, due to self-quenching in the aggregated state. Above the *cac*, the conjugate undergoes self-assembly in aqueous solution to form  $\beta$ -sheet structures as revealed by FTIR spectroscopy. The CD spectrum indicated chiral ordering of the FITC residues and it is presumed that strong  $\pi$ – $\pi$  stacking interactions

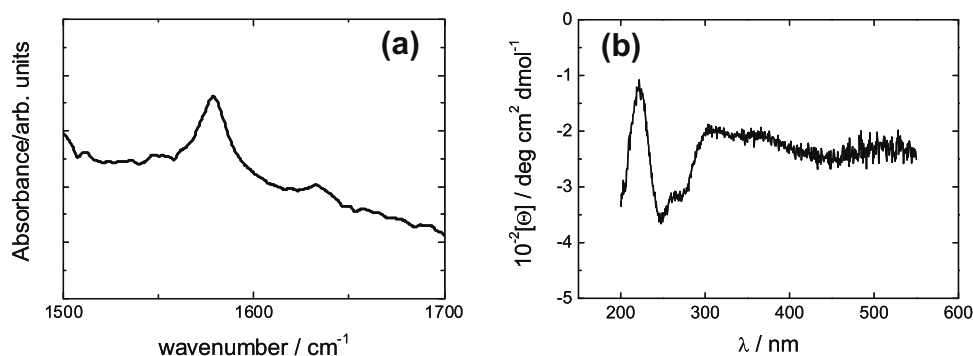


Fig. 4. Biophysical characterisation of FITC-LL. (a) FTIR spectrum obtained from an 0.73 wt% solution of FITC-LL, (b) CD spectrum from an 0.4 wt% solution of FITC-LL.

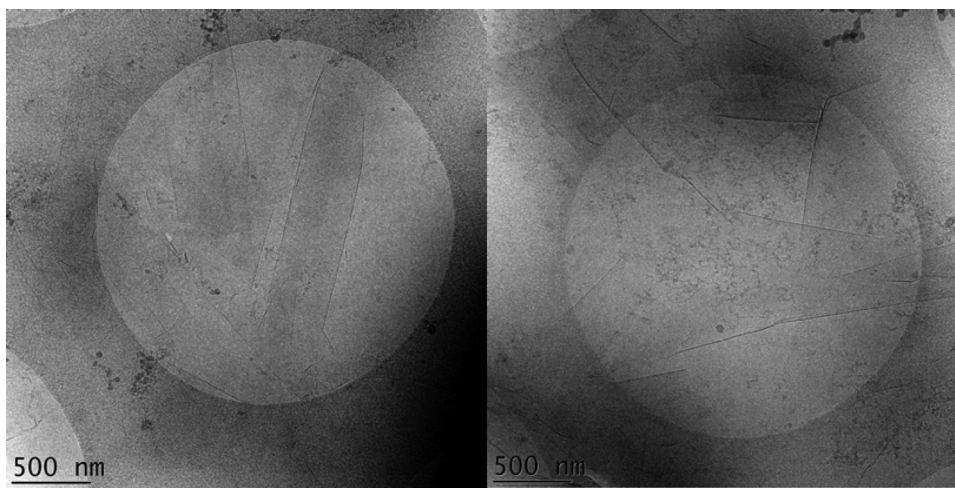


Fig. 5. Representative Cryo-TEM images obtained from a 0.73 wt% solution.

between these aromatic units plays an important driving role in the self-assembly process. Cryo-TEM and SAXS revealed that the self-assembled nanostructure comprises highly extended tapes based on a layered molecular stacking.

Our results show that FITC itself is not uptaken into cells but, remarkably, FITC-LL is readily uptaken by fibroblasts without any significant cytotoxicity. The molecular mechanism behind cell internalisation/uptake has yet to be elucidated but is a fascinating challenge for future research. Certainly, the peptide is too short to

correspond to a transporter sequence so another mechanism for uptake must be applicable. It is possible that self-assembly and cell uptake are correlated, for instance via local concentration enhancement of the conjugate in the vicinity of the cell membrane, although this needs further study. Regardless, the fluorophore-labelled self-assembled tapes may be useful in future biomaterials applications.

The novel conjugate FITC-LL shows excellent cytocompatibility, probed via live/dead cell assays using human fibroblasts, similar to that of FITC itself. It is shown to localise in the peri-nuclear region and in vesicle-shaped intracellular compartments. The marked absence of the PA from the nucleus proper might be explained by the fact that Nuclear Export Signals (NES) are necessarily leucine rich [50,51]. NES are responsible for actively exporting proteins from the nucleus to the perinuclear space. Thus it is tempting to speculate that FITC-LL localisation could be directed by NES and its associated machinery. Thus this conjugate represents a cytocompatible non-protein fluorophore in which, remarkably, the simple attached biocompatible dipeptide tag facilitates cell uptake, with potential utility for cell labelling applications.

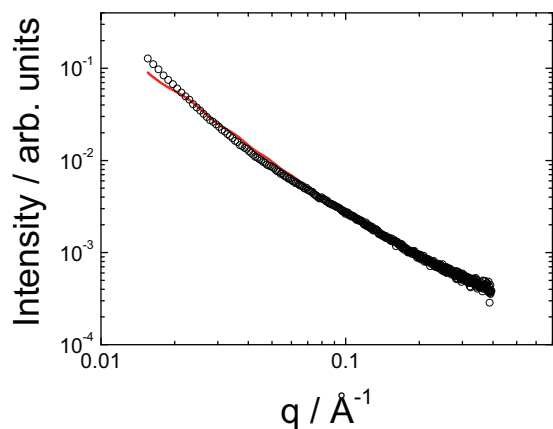


Fig. 6. SAXS intensity profile measured for a 0.5 wt% solution of FITC-LL (circles) along with a model bilayer form factor fit (red line). (For interpretation of the references to color in this figure legend, the reader is referred to the web version of this article.)

#### Acknowledgements

This research was supported by BBSRC grant BB/I008187/1 (CJC/IWH) and EPSRC grant EP/L020599/1 to IWH. We are grateful to Katsuaki Inoue and James Douch for assistance at Diamond (beamtime reference SM10007), to Emerson da Silva for the analysis of the *cac* data, and to Ashkan Dehsorkhi for assistance with SAXS measurements.

## Appendix A. Supplementary data

Supplementary data associated with this article can be found, in the online version, at <http://dx.doi.org/10.1016/j.colsurfb.2015.04.062>

## References

- [1] Y. Zhang, H. Gu, Z. Yang, B. Xu, Supramolecular hydrogels respond to ligand–receptor interaction, *J. Am. Chem. Soc.* 125 (2003) 13680–13681.
- [2] M. Reches, E. Gazit, Controlled patterning of aligned self-assembled peptide nanotubes, *Nat. Nanotechnol.* 1 (2006) 195–200.
- [3] Z. Yang, G. Liang, B. Xu, Enzymatic hydrogelation of small molecules, *Acc. Chem. Res.* 41 (2008) 315–326.
- [4] A.M. Smith, R.J. Williams, C. Tang, P. Coppo, R.F. Collins, M.L. Turner, A. Saiani, R.V. Ulijn, Fmoc-diphenylalanine self-assembles to a hydrogel via a novel architecture based on  $\pi$ - $\pi$  interlocked  $\beta$ -sheets, *Adv. Mater.* 20 (2008) 37–41.
- [5] D.M. Ryan, S.B. Anderson, B.L. Nilsson, The influence of side-chain halogenation on the self-assembly and hydrogelation of Fmoc-phenylalanine derivatives, *Soft Matter* 6 (2010) 3220–3231.
- [6] G. Cheng, V. Castelletto, C.M. Moulton, G.E. Newby, I.W. Hamley, Hydrogelation and self-assembly of Fmoc-tripeptides: unexpected influence of sequence on self-assembled fibril structure, and hydrogel modulus and anisotropy, *Langmuir* 26 (2010) 4990–4998.
- [7] D.J. Adams, Dipeptide and tripeptide conjugates as low-molecular-weight hydrogelators, *Macromol. Biosci.* 11 (2011) 160–173.
- [8] G. Cheng, V. Castelletto, R. Jones, C.J. Connon, I.W. Hamley, Hydrogelation of self-assembling RGD-based peptides, *Soft Matter* 7 (2011) 1326–1333.
- [9] V. Castelletto, C.M. Moulton, G. Cheng, I.W. Hamley, M.R. Hicks, A. Rodger, D.E. López-Pérez, G. Revilla-López, C. Alemán, Self-assembly of Fmoc-tetrapeptides based on the RGDS cell adhesion motif, *Soft Matter* 1140 (2011) 5–15.
- [10] B. Adhikari, G. Palui, A. Banerjee, Self-assembling tripeptide based hydrogels and their use in removal of dyes from waste-water, *Soft Matter* 5 (2009) 3452–3460.
- [11] S. Yuran, Y. Razvag, M. Reches, Coassembly of aromatic dipeptides into biomolecular necklaces, *ACS Nano* 6 (2012) 9559–9566.
- [12] L. Chen, K. Morris, A. Laybourn, D. Elias, M.R. Hicks, A. Rodger, L. Serpell, D.J. Adams, Self-assembly mechanism for a naphthalene-dipeptide leading to hydrogelation, *Langmuir* 2010 (2009) 5232–5242.
- [13] J. Zhou, X. Du, Y. Gao, J. Shi, B. Xu, Aromatic–aromatic interactions enhance interfiber contacts for enzymatic formation of a spontaneously aligned supramolecular hydrogel, *J. Am. Chem. Soc.* 136 (2014) 2970–2973.
- [14] Y. Kuang, Y. Gao, J. Shi, J. Li, B. Xu, The first supramolecular peptidic hydrogelator containing taurine, *Chem. Commun.* 50 (2014) 2772–2774.
- [15] M.L. Ma, Y. Kuang, Y. Gao, Y. Zhang, P. Gao, B. Xu, Aromatic–aromatic interactions induce the self-assembly of pentapeptidic derivatives in water to form nanofibers and supramolecular hydrogels, *J. Am. Chem. Soc.* 132 (2010) 2719–2728.
- [16] B. Adhikari, J. Nanda, A. Banerjee, Pyrene-containing peptide-based fluorescent organogels: inclusion of graphene into the organogel, *Chem. Eur. J.* 17 (2011) 11488–11496.
- [17] S. Fleming, S. Debnath, P.W.J.M. Frederix, N.T. Hunt, R.V. Ulijn, Insights into the coassembly of hydrogelators and surfactants based on aromatic peptide amphiphiles, *Biomacromolecules* 15 (2014) 1171–1184.
- [18] J. Li, Y. Kuang, Y. Gao, X. Du, J. Shi, B. Xu, D-amino acids boost the selectivity and confer supramolecular hydrogels of a nonsteroidal anti-inflammatory drug (NSAID), *J. Am. Chem. Soc.* 135 (2012) 542–545.
- [19] Y. Gao, Y. Kuang, X. Du, J. Zhou, P. Chandran, F. Horkay, B. Xu, Imaging self-assembly dependent spatial distribution of small molecules in a cellular environment, *Langmuir* 29 (2013) 15191–15200.
- [20] J.Y. Li, Y. Kuang, Y. Gao, X.W. Du, J.F. Shi, B. Xu, D-amino acids boost the selectivity and confer supramolecular hydrogels of a nonsteroidal anti-inflammatory drug (NSAID), *J. Am. Chem. Soc.* 135 (2013) 542–545.
- [21] J. Li, Y. Kuang, J. Shi, Y. Gao, J. Zhou, B. Xu, The conjugation of nonsteroidal anti-inflammatory drugs (NSAID) to small peptides for generating multifunctional supramolecular nanofibers/hydrogels, *Beilstein J. Org. Chem.* 9 (2013) 908–917.
- [22] J.Y. Li, Y. Gao, Y. Kuang, J.F. Shi, X.W. Du, J. Zhou, H.M. Wang, Z.M. Yang, B. Xu, Dephosphorylation of D-peptide derivatives to form biofunctional, supramolecular nanofibers/hydrogels and their potential applications for intracellular imaging and intratumoral chemotherapy, *J. Am. Chem. Soc.* 135 (2013) 9907–9914.
- [23] F. Zhao, M.L. Ma, B. Xu, Molecular hydrogels of therapeutic agents, *Chem. Soc. Rev.* 38 (2009) 883–891.
- [24] Z. Yang, H. Gu, D. Fu, P. Gao, J.K.W. Lam, B. Xu, Enzymatic formation of supramolecular hydrogels, *Adv. Mater.* 16 (2004) 1440–1444.
- [25] V. Jayawarna, M. Ali, T.A. Jowitt, A.F. Miller, A. Saiani, J.E. Gough, R.V. Ulijn, Nanostructured hydrogels for three-dimensional cell culture through self-assembly of fluorenylmethoxycarbonyl-dipeptides, *Adv. Mater.* 18 (2006) 611–614.
- [26] M. Zhou, A.M. Smith, A.K. Das, N.W. Hodson, R.F. Collins, R.V. Ulijn, J.E. Gough, Self-assembled peptide-based hydrogels as scaffolds for anchorage-dependent cells, *Biomaterials* 30 (2009) 2523–2530.
- [27] D.J. Adams, P.D. Topham, Peptide conjugate hydrogelators, *Soft Matter* 6 (2010) 3707–3721.
- [28] K. Montrose, Y. Yang, X.Y. Sun, S. Wiles, G.W. Krissansen, Xentry, a new class of cell-penetrating peptide uniquely equipped for delivery of drugs, *Sci. Rep.* 3 (2013).
- [29] R.P. Haugland, *The Handbook – A Guide to Fluorescent Probes and Labeling Technologies*, Molecular Probes, Eugene, Oregon, 2005.
- [30] B.N.G. Giepmans, S.R. Adams, M.H. Ellisman, R.Y. Tsien, Review – the fluorescent toolbox for assessing protein location and function, *Science* 312 (2006) 217–224.
- [31] P. Zhang, A.G. Cheetham, L.L. Lock, H. Cui, Cellular uptake and cytotoxicity of drug–peptide conjugates regulated by conjugation site, *Bioconj. Chem.* 24 (2013) 604–613.
- [32] P. Zhang, L.L. Lock, A.G. Cheetham, H. Cui, Enhanced cellular entry and efficacy of Tat conjugates by rational design of the auxiliary segment, *Mol. Pharm.* 11 (2014) 964–973.
- [33] H. Choi, S.R. Choi, R. Zhou, H.F. Kung, I.W. Chen, Iron oxide nanoparticles as magnetic resonance contrast agent for tumor imaging via folate receptor-targeted delivery, *Acad. Radiol.* 11 (2004) 996–1004.
- [34] C.W. Lu, Y. Hung, J.K. Hsiao, M. Yao, T.H. Chung, Y.S. Lin, S.H. Wu, S.C. Hsu, H.M. Liu, C.Y. Mou, C.S. Yang, D.M. Huang, Y.C. Chen, Bifunctional magnetic silica nanoparticles for highly efficient human stem cell labeling, *Nano Lett.* 7 (2007) 149–154.
- [35] M. Huang, E. Khor, L.Y. Lim, Uptake and cytotoxicity of chitosan molecules and nanoparticles: effects of molecular weight and degree of deacetylation, *Pharm. Res.* 21 (2004) 344–353.
- [36] C.B. He, Y.P. Hu, L.C. Yin, C. Tang, C.H. Yin, Effects of particle size and surface charge on cellular uptake and biodistribution of polymeric nanoparticles, *Biomaterials* 31 (2010) 3657–3666.
- [37] N. Murthy, J. Campbell, N. Fausto, A.S. Hoffman, P.S. Stayton, Design and synthesis of pH-responsive polymeric carriers that target uptake and enhance the intracellular delivery of oligonucleotides, *J. Control. Release* 89 (2003) 365–374.
- [38] O. Aronov, A.T. Horowitz, A. Gabizon, D. Gibson, Folate-targeted PEG as a potential carrier for carboplatin analogs. Synthesis and in vitro studies, *Bioconj. Chem.* 14 (2003) 563–574.
- [39] S.S. Twining, Fluorescein-isothiocyanate casein assay for proteolytic enzymes, *Anal. Biochem.* 143 (1984) 30–34.
- [40] S. Izumi, Y. Urano, T. Hanaoka, T. Terai, T. Nagano, A simple and effective strategy to increase the sensitivity of fluorescence probes in living cells, *J. Am. Chem. Soc.* 131 (2009) 10189–10200.
- [41] B. Stuart, *Biological Applications of Infrared Spectroscopy*, Wiley, Chichester, 1997.
- [42] I.W. Hamley, Peptide fibrillation, *Angew. Chem.* 46 (2007) 8128–8147.
- [43] C. Toniolo, F. Formaggio, R.W. Woody, Electronic circular dichroism of peptides, in: N. Berova, P.L. Polavarapu, K. Nakanishi, R.W. Woody (Eds.), *Comprehensive Chiroptical Spectroscopy*, vol. 2, 2012, New York.
- [44] J.R. Lakowicz, *Principles of Fluorescence Spectroscopy*, Kluwer, New York, 1999.
- [45] <http://www.fluorophores.tugraz.at/substance/252>, 2015.
- [46] V. Castelletto, G. Cheng, C. Stain, C.J. Connon, I.W. Hamley, Self-assembly of a peptide amphiphile containing L-carnosine and its mixtures with a multilamellar vesicle forming lipid, *Langmuir* 28 (2012) 11599–11608.
- [47] I.W. Hamley, A. Dehsorkhi, V. Castelletto, Self-assembled arginine-coated peptide nanosheets in water, *Chem. Commun.* 49 (2013) 1850–1852.
- [48] V. Castelletto, R.J. Gouveia, C.J. Connon, I.W. Hamley, New RGD-peptide amphiphile mixtures containing a negatively charged diluent, *Faraday Discuss.* 166 (2013) 381–397.
- [49] <http://kur.web.psi.ch/sans1/SANSSoft/sasfit.html>, 2015.
- [50] U. Fischer, J. Huber, W.C. Boelens, I.W. Mattaj, R. Luhrmann, The HIV-1 REV activation domain is a nuclear export signal that accesses an export pathway used by specific cellular RNAs, *Cell* 82 (1995) 475–483.
- [51] W. Wen, J.L. Meinkoth, R.Y. Tsien, S.S. Taylor, Identification of a signal for rapid export of proteins from the nucleus, *Cell* 82 (1995) 463–473.